Bioresource Technology 135 (2013) 283–291

Contents lists available at SciVerse ScienceDirect

Bioresource Technology

journal homepage: www.elsevier.com/locate/biortech

Pilot-scale chemical–biological system for efficient H_2S removal from biogas

Wei-Chih Lin, Yu-Pei Chen, Ching-Ping Tseng *

Department of Biological Science and Technology, National Chiao Tung University, Hsinchu 300, Taiwan

HIGHLIGHTS

- We have constructed a pilot scale chemical–biological H_2S removal system.
- This system had operated consecutive 356-d for livestock biogas purification.
- The purified biogas was collected for power generation by a 30 kW biogas generator.
- This system performed robustly in operation and is a feasible for biogas cleaning.

ARTICLE INFO

Article history:
Available online 22 October 2012

Keywords:
Biogas
H_2S
Pilot scale
Acidithiobacillus ferrooxidans
Power generation

ABSTRACT

A pilot-scale chemical–biological process was performed efficiently to remove corrosive H_2S from biogas. Consecutive 356-d livestock biogas purification was conducted at various H_2S loading rates. The average inlet H_2S concentration was 3542 ppm, and a removal efficiency of 95% was achieved with gas retention time of 288 s. This system showed robust performance during operation with stable parameters. Purified biogas with an average of 59% CH_4 was collected for power production. Moreover, 28.3 kW h of power was produced by using a 30 kW biogas generator under 300 LPM biogas flow rate. During the 30-d shut down test, the jarosite formation resulted in pH decrease and appearance of *Leptospirillum* sp. and *Sulfobacillus* sp. in the bioreactor. However, the cell density of the inoculated *Acidithiobacillus ferrooxidans* was maintained above 5×10^7 CFU/g-AC during long-term operation. Thus, given the successful H_2S elimination, the chemical–biological process is a feasible system for biogas purification.

1. Introduction

Biogas is anaerobically produced from the digestion of organic objects or other biodegradable feedstock. The components of biogas vary depending on the substrate (Rasi et al., 2007). For instance, biogas obtained by digesting swine-slurry wastewater generally contains approximately 65–75% CH_4, 25–35% CO_2, 3000–8000 ppm H_2S, and traces of N_2 and NH_3. The high heating value of CH_4 (37.78 MJ/m^3) makes biogas a good renewable energy source (Nizami and Murphy, 2010). With regards to the global warming issue, the combustion of methane produces less carbon dioxide per unit of heat released than any other hydrocarbon fuel (Demirbas, 2010). In addition to heat or power generation, several studies introduced biogas for microalgal growth, the process of which utilizes the carbon dioxide captured in the culture media. The microalgal biomass is subsequently processed to produce biodiesel, dietary supplements, and animal feeds (Chiu et al., 2011). However, failure to eliminate the corrosive and toxic H_2S in raw biogas has been the drawback of many biogas applications.

A number of H_2S elimination techniques are conducted based on physical (Belmabkhout et al., 2009), chemical (Peiffer and Gade, 2007), or biological (Chung et al., 2007; Gabriel, 2003) principles. Physical methods such as membrane separation, water scrubbing, and active carbon processes are rapid and effective, but are not economical for frequent media replacement that is required when dealing with high H_2S loading elimination (Chung et al., 2007). Chemical methods require the addition of chemicals (e.g., NaOH or iron salts), which are costly, unhealthy, and produce secondary wastes. Moreover, some chemical regeneration processes are dangerous (e.g., large amounts of heat produced during iron oxide regeneration). Thus, several studies explored the advantages of biological methods. Acidophile microbes, such as *Acidithiobacillus thiooxidans* (Ramírez et al., 2011) and neutrophile microbes, such as *Thiobacillus thioparus* (Chung et al., 2007) and *Pseudomonas* sp. (Ho et al., 2008), were utilized to convert H_2S directly into sulfate or sulfur. These chemoautotrophic microbes maintained a dominant population during long-term operation, and facilitated the economical and easy handling of the derived bioreactor. However, the toxic tolerance of microbes subjected to high H_2S loading and

* Corresponding author. Address: Department of Biological Science and Technology, National Chiao Tung University, 75 Bo-Ai Street, Hsin-Chu, Taiwan. Tel.: +886 3 5731596; fax: +886 3 5729288.
E-mail address: cpts@cc.nctu.edu.tw (C.-P. Tseng).

0960-8524/$ - see front matter © 2012 Elsevier Ltd. All rights reserved.
http://dx.doi.org/10.1016/j.biortech.2012.10.040

the steep decrease in pH during sulfate accumulation are the main drawbacks identified.

In a system that combines chemical and biological methods to remove H_2S, the gas is first oxidized by ferric iron to generate elemental sulfur in a chemical reactor. The resulting ferrous iron is then oxidized by iron-oxidizing bacteria, such as *A. ferrooxidans* or *Leptospirillum ferrooxidans* (Dave, 2008) in the biological reactor. Several studies were conducted to determine the optimal culture conditions of *A. ferrooxidans* to obtain the optimal ferrous iron oxidation rate because biological oxidation is the rate-limiting step in this closed circulation system (Malhotra et al., 2002; Mesa et al., 2002). The growth conditions of *A. ferrooxidans* include pH 1.5–2.0, incubation temperatures between 30 °C and 35 °C, and a ferrous iron concentration ranging from 10 g/L to 20 g/L. In addition, alternative supporting materials and processes for microbe immobilization have been proposed to evaluate different types of biological systems for continuous ferrous iron oxidation using *A. ferrooxidans* and *L. ferrooxidans* (Giaveno et al., 2008; Park et al., 2005). Chung et al. (2006) suggested that the addition of an extra carbon source (less than 0.1% glucose) enhances *A. ferrooxidans* growth and ferrous iron oxidation.

Other studies focused on the optimal parameters in the chemical H_2S oxidation process. The efficiency of H_2S absorption substantially increases with both increasing pH and ferric iron concentration (Nielsen et al., 2008). The kinetic models of H_2S absorption by aqueous ferric sulfate were also studied (Ebrahimi et al., 2003). In addition, the chemical reactor (absorber) design used is a significant subject for a robust pilot-scale biochemical biogas purification system for long-term operation. Giro et al. (2006) filled small PVC (polyvinyl chloride) cylinders in the absorber to enhance H_2S removal efficiency. The H_2S was then introduced from the bottom of the reactor and was oxidized by the iron solution that trickled from the top. Furthermore, Chung et al. (2006) soaked the glass beads in an iron solution in the absorber and introduced H_2S from the bottom. Although these reactors performed well on a bench scale, no practical utilization for biogas treatment on a pilot scale has been published.

In this study, a pilot-scale chemical–biological system for biogas purification was constructed on a swine farm. Using an alternative H_2S absorber design, three hollow absorbers in a serial connection were attached to this system for H_2S elimination. The iron solution was sprayed out from the nozzles at the top of the absorbers to react with the biogas. Biogas with an average concentration of 3542 ppm H_2S was purified at a gas retention time (GRT) range of 48–288 s (biogas flow rate at 50–300 liter per minute (LPM)) throughout a 356-d experiment to evaluate the performance of the combined system. The purified biogas was collected for power production by a 30 kW biogas generator. The parameters, which include H_2S loading, ferrous and ferric iron concentrations, bioreactor incubation temperatures, pressure drop, and cell count, were periodically evaluated. The analysis of the microbial population in the bioreactor was also monitored by denaturing gradient gel electrophoresis (DGGE) during the operation. The pilot-scale chemical–biological system can effectively remove H_2S and can be a feasible method for biogas purification.

2. Methods

2.1. Microorganism cultivation and immobilization

A. ferrooxidans CP9 was isolated from an acid mine drainage and was identified by 16S rRNA gene cloning and sequencing (GenBank accession number EF605251). The pure strain was grown in a 9K medium at 30 °C. The medium contained (L^{-1}) 3 g $(NH_4)_2SO_4$, 0.5 g K_2HPO_4, 0.5 g $MgSO_4{\cdot}7H_2O$, 0.1 g/L KCl, 0.01 g $Ca(NO_3)_2$, and 100 g $FeSO_4{\cdot}7H_2O$. The number of *A. ferrooxidans* CP9 cells was determined by preparing 9K solid medium containing (L^{-1}) 3 g $(NH_4)_2SO_4$, 0.5 g K_2HPO_4, 0.5 g $MgSO_4{\cdot}7H_2O$, 0.1 g/L KCl, 0.01 g $Ca(NO_3)_2$, 22 g $FeSO_4{\cdot}7H_2O$, and 10 g agar (Chung et al., 2006). Granular activated carbon (GAC; China Activated Carbon Industries Ltd., Taiwan) was used to immobilize the *A. ferrooxidans* CP9 in the bioreactor as described previously (Chung et al., 2006).

2.2. Combining chemical and bioreactors for biogas purification in pilot scale

The scheme of the chemical–biological biogas purification system is shown in Fig. 1. Three hollow H_2S absorbers (25 cm $\Phi \times$ 160 cm H) in serial connection were equipped with stainless steel nozzles. The size of bioreactor was 120 cm $\Phi \times$ 200 cm H. Two storage tanks (1000 L each) were serially connected between the biological and chemical reactors.

The raw biogas produced from the swine wastewater treatment was collected in the PVC textile bag (Nan YA Plastic Corporation, Taiwan). The H_2S in the biogas that was introduced into the first absorber was oxidized to sulfur by the ferric iron solution sprayed out from the nozzle in reverse direction. The biogas filtered from the first absorber was then sequentially introduced into the second and third absorbers. The elemental sulfur formed at the three absorbers was flushed into the first storage tank and precipitated. The clearer solution in the second tank was periodically pumped into the bioreactor for medium circulation at a rate of 1440 L/d. A spraying pump pressed the solution into the absorbers for biogas purification. This system was operated at 30 min per hour and 12 h per day. The purified biogas fitting the criterion of having an H_2S concentration below 150 ppm was collected and used in the power production stage using a 30 kW biogas generator.

2.3. Analytical methods

The inlet and outlet H_2S concentrations were measured using a gas detector tube with a gas-sampling pump (AP-20, Komyo Rika-Gaku Kogyo, Japan). The ferrous iron, ferric iron, and total iron concentrations were determined as described previously (Chung et al., 2006). The pH and temperature of the solution in the bioreactor was measured with a portable pH meter. For cell count analyses, the microbes were routinely removed from GAC that were collected at a depth of 20 cm in the bioreactor sampling port and cultured on the solid 9K. The dark-brown colony in the medium was indicated as *A. ferrooxidans* CP9 after 7–14 d of incubation. Gas retention time (GRT) was evaluated using the following equation:

$$GRT = V/Q$$

where GRT is the gas retention time (min), V is the volume of the total number of absorbers (L), and Q is the gas flow rate (L/min).

H_2S loading (g-S/m^3/h) based on the absorbers was evaluated using the following equation:

$$loading = (Q \times C)/V$$

where Q is the gas flow rate (L/h), C is the inlet concentration (g-S/L), and V is the volume of the total number of absorbers (m^3).

The biological oxidation rate (g-Fe/L/d) was calculated using the following equation:

$$Oxidation\ rate = ((C_o — C_i) \times Q')/V'$$

where Q' is the medium circulation rate (L/d), C_o is the ferric iron concentration of the medium leaving the bioreactor (g/L), C_i is the ferric iron concentration of the medium flow into the bioreactor (g/L), and V' is the total medium volume in the bioreactor (L).

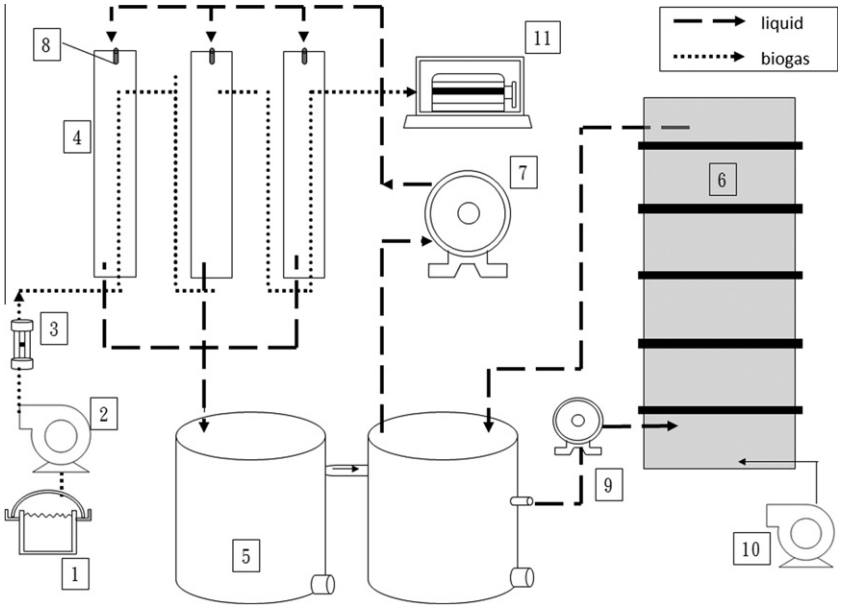

Fig. 1. Schematic diagram of the experimental apparatuses used: (1) anaerobic digester; (2) biogas blower; (3) biogas flow meter; (4) chemical absorbers; (5) medium storage tanks; (6) biological reactor; (7) spraying pump; (8) spraying nozzles; (9) liquid pump; (10) air compressor; and (11) 30 kW biogas power generator.

2.4. Bacterial community analysis

Sample treatment and genomic DNA extraction were performed as described by Ho et al. (2008). The nested PCR was performed to increase the amount of PCR products obtained. The first set of primers (9F: 5′-gag ttt gat cct ggc tca g-3′; 1543R: 5′-aga aag gag gtg atc cag c-3′) was used for the following first-stage PCR procedure: 2 min at 95 °C, followed by 30 cycles of 30 s at 95 °C, 30 s at 60 °C, and 90 s at 72 °C, concluding with a 10 min incubation at 4 °C. The PCR product was then used as the template for the second-stage PCR. The GC clamped primers (341F-GC: 5′-cgc ccg ccg cgc ccc gcg ccc gtc ccg ccg ccc ccg ccc gcc tac ggg agg cag cag-3′; 907R: ccg tca att cmt ttg agt tt) were applied using the following procedure: 2 min at 95 °C, followed by 28 cycles of 30 s at 95 °C, 30 s at 64 °C, and 40 s at 72 °C, concluding with a 10 min incubation at 4 °C.

The samples were then run on an 8% acrylamide gel with a 45–60% denaturant gradient using a Bio-Rad DGGE apparatus. The electrophoresis procedure, staining, and rinsing were performed as described by Ho et al. (2008). The desired fragments were excised from DGGE gels for DNA sequencing. The BLASTN program was used to search for nucleotide sequence similarities on the NCBI website.

3. Results and discussion

3.1. Effect of inlet H_2S concentration and loading on the performance of combined chemical–biological reactor

During the 356-d pilot-scale operation, the biogas produced from the anaerobic fermentation of swine wastewater treatment was introduced into the chemical–biological H_2S elimination system at various gas retention times (GRT). Fig. 2 shows the H_2S inlet/outlet concentrations and removal performance at different operational stages. The average H_2S, CH_4, and CO_2 inlet concentrations during the operation were 3542 ppm, 59%, and 21%, respectively.

The shock loading and recovery test were conducted at stages 4 and 5. When an excess amount of 300 LPM biogas inlet rate with an average H_2S loading of 212.6 g-S/m^3/h was introduced, the removal efficiency dropped from 97% to 65% within 10 d. The ferrous iron oxidation rate was insufficient and was unable to compensate for the rapid ferric iron consumption. However, when the biogas inlet rate was adjusted back to 100 LPM at the recovery stage, the removal efficiency increased up to 90% within 2 weeks. Thus, this system was not permanently damaged by sudden spikes in H_2S loading and can be reliably used with various inlet H_2S concentrations.

Fig. 3A illustrates the H_2S loadings and oxidation ability of iron in the chemical absorber. In the first three stages, the inlet flow rates were kept at 150, 50, and 100 LPM with GRTs of 1.6, 4.8, and 2.4 min, respectively. The maximum average elimination capacity (EC) was 79.4 g-S/m^3/h, whereas the removal efficiency was 87.1% at the first stage. The average removal efficiencies of 94.7% and 94.8% were obtained in stages 2 and 3, respectively, with EC values of 26.7 and 63.6 g-S/m^3/hr. Thus, higher removal efficiency could be attained with less EC.

When the H_2S content was less than 150 ppm, the residual H_2S was not easily removed by the chemical absorber. Thus, a mass transfer barrier existed in the rear part of the serially connected chemical absorbers. Nevertheless, a low H_2S content at 150 ppm is sufficient in combined heat and power generation (500 ppm) and for internal combustion gas engines (150 ppm) (Soreanu et al., 2010). In the present study, the purified biogas with an average residual H_2S content of 313 ppm was introduced into the storage bag. The residual H_2S was further reduced to less than 50 ppm after moisture elimination. The purified biogas was processed for power production by a 30 kW biogas power generator. A 300 LPM biogas flow rate (fuel/air ratio = 0.2) with an average of 59% CH_4 concentration produced 28.3 kW h of power.

When H_2S loading and the corresponding elimination capacity were plotted in Fig. 3B, a linear relationship was obtained for the operation except for the shock loading stage. The removal capacity was slightly decreased 6.8% at 150 LPM compared with a 100 LPM flow rate. However, the removal capacity decreased 22% when the flow rate was at 300 LPM. Furthermore, all the removal efficiencies were above 95% below 79 g-S/m^3/h loading.

In this study, the daily treated biogas volume and H_2S loading were 72 m^3 and 355 g, respectively, at a flow rate of 100 LPM.

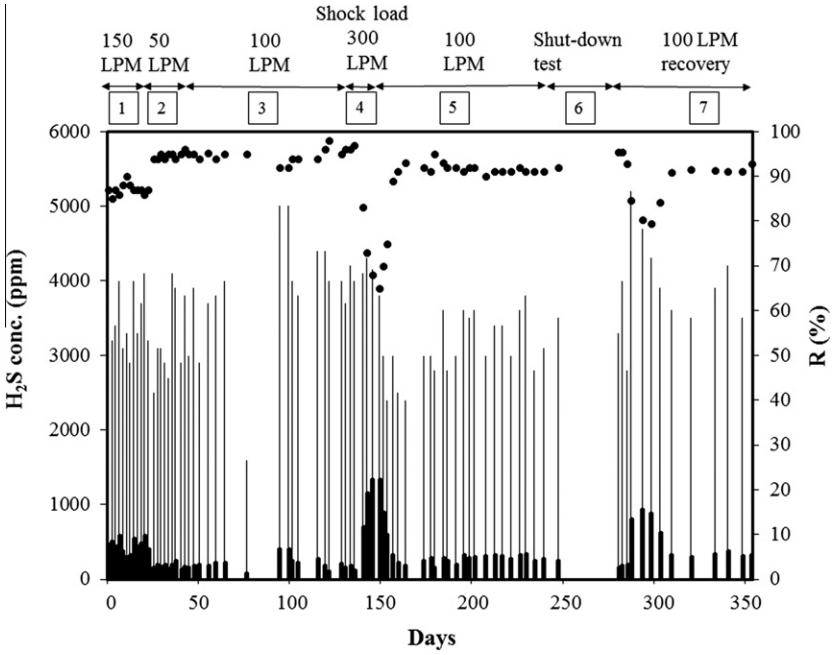

Fig. 2. H_2S inlet/outlet concentration and removal performance in the seven operational stages. The thin line and bold line indicate the H_2S inlet and outlet concentrations, respectively. The solid circles represent the H_2S removal efficiencies. The biogas flow rates were adjusted in different stages.

The scale of this study was much higher than that of biogas purification in previous reports. The biotrickling filter (1 m^3 biogas and 2.8 g H_2S loading) proposed by Soreanu et al. (2010), the anaerobic sludge bioreactor (0.1 m^3 biogas and 0.2 g H_2S loading) proposed by Deng et al. (2009), and the biotrickling filter (1.2 m^3 biogas and 5.8 g H_2S loading) proposed by Tanaka (2002) are discussed. Few studies on ambient wastewater odor treatment were published, and these studies used larger treatment scales than the present study. Omri et al. (2011) operated a sludge-based biofiltration system where a treated gas volume of 2880 m^3/d and an H_2S loading of 596–2990 g/d were processed. Gabriel (2003) operated a biotrickling filter with a treated gas volume of 16,300 m^3/h and an H_2S loading of 113–566 g/h. However, the inlet H_2S concentrations in these studies were only 149–746 ppm and 5–25 ppm, respectively.

Furthermore, in this study, Raching rings (with specific area 21 m^2/m^3) were also used to pack in the absorbers with a height of 30 cm based on a previous study (Mesa et al., 2004). Nevertheless, for loadings between 40 and 60 g-S/m^3/h, the formed sulfur precipitate clogged the absorber in the packed zone within 15 d (data not shown). Therefore, packing materials in the absorber of the chemical–biological combined system could become an obstruction.

3.2. Fe^{2+}/Fe^{3+} ratio variation in the chemical–biological system

In the chemical–biological combined system, the ferric iron concentration was directly proportional to the H_2S removal efficiency (Pagella and De Faveri, 2000). The Fe^{2+}/Fe^{3+} concentrations were determined during the operation to explore further the relationships among iron concentration, biological oxidation ability, and H_2S removal rate. The biological iron oxidation ability was calculated and corresponded with the H_2S inlet loading (Fig. 3A). The high H_2S loading led to rapid ferrous iron production in the chemical reactor, and resulted in the high oxidation activity of *A. ferrooxidans* in the biological reactor. These results were in agreement with the observations by Mesa et al. (2002) in bench scale studies where *A. ferrooxidans* achieved a higher oxidation rate of ferrous iron at 15 g/L compared with 10 and 5 g/L in continuous culture.

Fig. 4A and B shows the ferrous and ferric ion concentrations sampled from the outlets of the storage tank and bioreactor, respectively. The short GRT resulted in a high H_2S loading and led to the accumulation of ferrous iron. At the shock loading stage with 300 LPM, the rapid decrease of ferric iron from 11 to 4 g/L in the storage tank resulted in decreased removal efficiency. By contrast, a stable H_2S elimination rate was observed in stage 2 at 50 LPM, whereas ferric iron was stably accumulated. Thus, 92% removal efficiency was reached when the ferric iron concentration was maintained at 9.5 g/L.

When the inlet loading was ceased in the shutdown stage, the amount of ferric iron increased to 18 g/L in 20 d. This value was maintained until the restart of the system. The ferric iron concentration progressively increased because *A. ferrooxidans* are unable to utilize ferric iron as an electron acceptor in aerobic conditions (Kucera et al., 2011). Moreover, the biological oxidation ability weakened during the shutdown period and the first 16 d of the recovery period, which resulted in the rapid decrease of the ferric iron concentration to 7.8 g/L and the removal rate decreased to 80% early in stage 7. However, the oxidation ability of *A. ferrooxidans* was restored, and the ferric iron concentration increased above 10 g/L in the next 15 d. Thus, the bioreactor achieved a high recovery rate after 30 d of shutdown test.

3.3. pH and pressure drop variation during the operation processes

H_2S was absorbed and oxidized to elemental sulfur in this chemical–biological removal system. In the conditions of 100 LPM of inlet biogas with 4000 ppm H_2S, 400 g of sulfur was produced every day in this system. Although the two sequentially connected storage tanks were set up, trace sulfur could still enter the bioreactor along with the circulation medium. In addition to sulfur, the formation of biofilm or ferric hydroxide might result in clogging or the appearance of an anaerobic zone when air was introduced during intermittent shutdown.

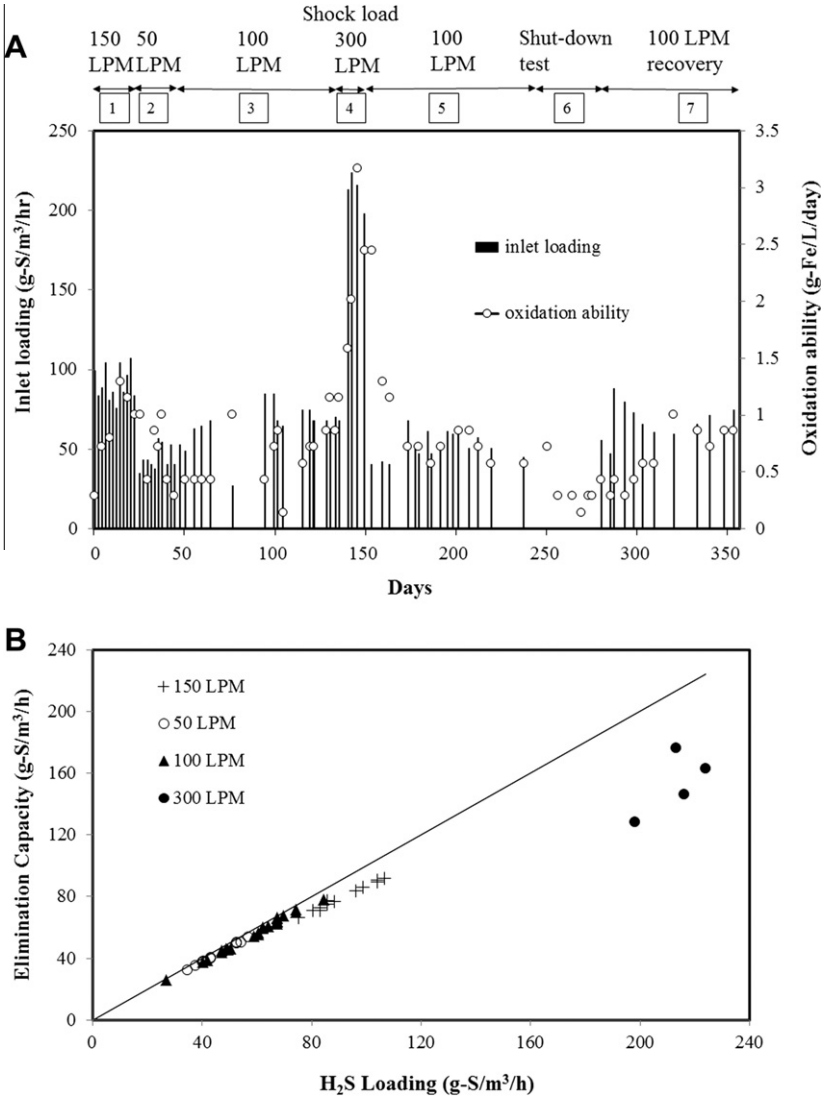

Fig. 3. Effects of H_2S loadings on the system performance. (A) H_2S loadings in the chemical absorber and the ferrous iron oxidation ability of the biological reactor. (B) Plot of the H_2S loading and the corresponding elimination capacity. The line represents 100% elimination reference. The biogas flow rate 150 LPM (cross) was conducted in the stage 1; 50 LPM flow rate (open circle) was conducted in stage 2; 100 LPM flow rate (triangle) was conducted in stage 3, stage 5 and stage 7; 300 LPM flow rate (solid circle) was conducted in stage 4 (the shock loading).

Fig. 5A shows the pressure drop and pH variation profiles at each stage. In the immobilization period, the pressure drop was constantly sustained at 22 mmH_2O/m. In stages 1–5, the pressure drop slightly increased at an average rate of 0.75 mmH_2O/m per week on the 250 d of operation. No significant elevation was observed even during the peak loading.

However, the rapid increase in pressure drop was observed during the shutdown test at an average of 3.23 mmH_2O/m per week because of proton consumption in the biological reactor. When ferrous iron was continuously oxidized without the counteraction from H_2S oxidation, the number of protons was suggested decreased in the beginning of stage 6. In high pH conditions, ferric iron was inclined toward a hydrolytic reaction and produced ferric hydroxide precipitate and protons (Pagella and De Faveri, 2000; Sharma, 2003). The pH was observed continuously dropped to 1.38 in the next 25 d. Furthermore, another precipitation formation reaction competed with the hydrolysis reaction and produced basic ferric hydroxysulphate (jarosite) with the formula $MFe_3(SO_4)_2(OH)_6$, where M might be K^+, Na^+, NH_4^+, Ag^+, or H_3O^+ (Daoud and Karamanev, 2006). These hydroxysulphate precipitates formed in the bioreactor could also cause the pH decrease and the increase in pressure drop. By the consumption of ferrous iron, the energy source in the bioreactor was switched from ferrous iron to sulfur which led *A. ferrooxidans* CP9 to produce sulfate and decreased the pH during the shutdown test. The similar result was also observed in lab scale energy source switch test in previous study (Yarzabal, 2004).

In the recovery period of stage 7, the pH stopped decreasing and the pressure drop increase was slowed. Thus, the recovery of H_2S oxidation may have resulted in the elevation of ferrous iron concentration. The Fe^{2+}/Fe^{3+} concentration balance could contribute to a stable environmental pH and is essential for the chemical–biological process. In many biological H_2S elimination processes, the negative effects of low pH caused by sulfate accumulation inhibit cell growth and its oxidation ability. The continuous addition of several alkaline chemicals, such as $NaHCO_3$ (Jiang et al., 2009) or NaOH (González-Sánchez et al., 2008), to adjust the pH was necessary in long-term operations. Therefore, the stable pH during H_2S elimination in this system was an advantage compared with other methods, which directly metabolize H_2S to sulfate by sulfide oxidizing bacteria.

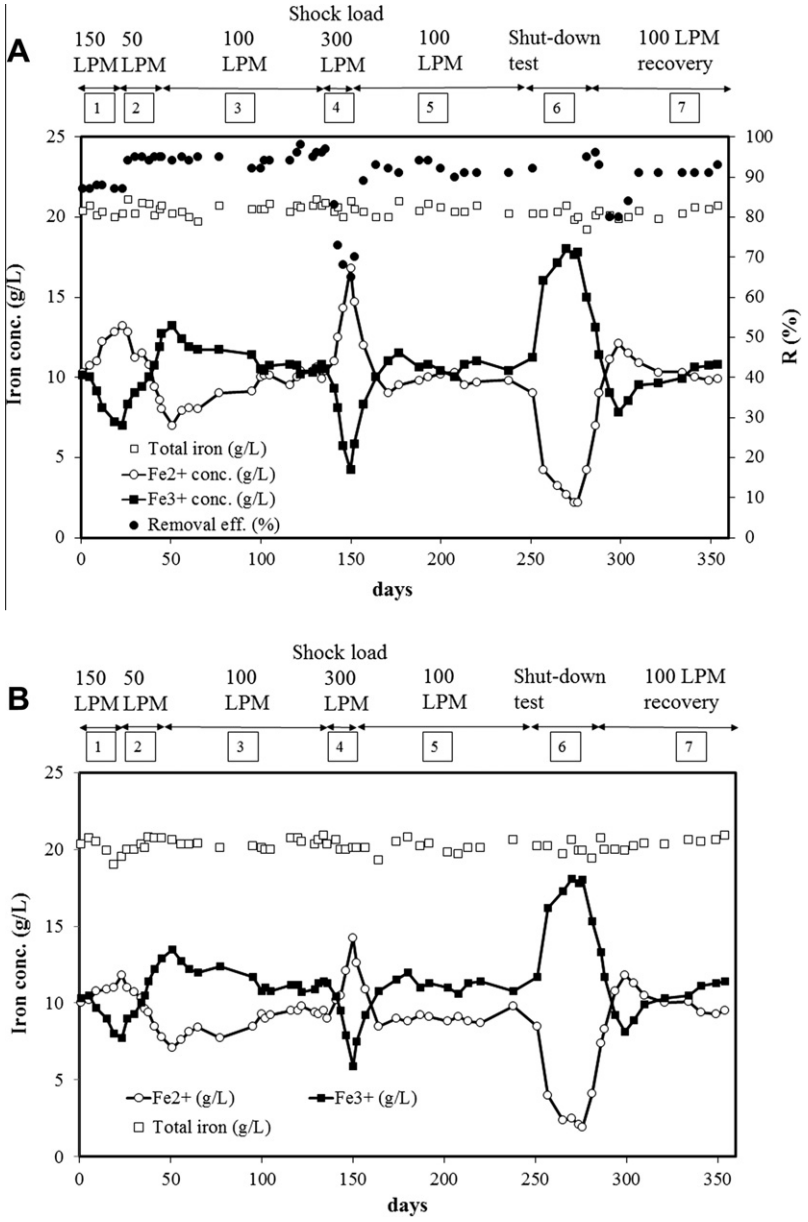

Fig. 4. Ferrous, ferric, and total iron concentrations in the (A) storage tank and (B) biological reactor.

3.4. Bacterial cell numbers and community analysis

The oxidation ability and cell growth of *A. ferrooxidans* is temperature-dependent. Through bench scale studies, we found that the cell counts of *A. ferrooxidans* CP9 decreased to 50% and 85% at 18 °C and 42 °C, respectively, compared with that at 35 °C in the bioreactor (data not shown). Malhotra et al. (2002) found that the cell count and ferrous iron oxidation rate increased with increasing temperature, specifically, from 5 °C to 37 °C. In the present study, the cell counts and temperatures in the bioreactor were routinely determined.

Fig. 5B shows that the H_2S elimination system began when the cell count reached 2×10^8 CFU/g-AC. The cell growth was not affected by the intensity of H_2S loading during the first five stages in the 250 d of operation, whereas the cell number varied between 1.4×10^8 CFU/g-AC to 6.9×10^8 CFU/g-AC. The slight decrease in cell count was assumed caused by the temperature drop.

However, the cell count decreased to one-tenth of the original value after the depletion of ferrous iron during the shutdown period. Nevertheless, the cell count in the suspension media of the bioreactor increased 1000-fold, compared with those at the earlier stages in the 250 d of operation (data not shown). Previous studies (He et al., 2008) have shown that *A. ferrooxidans* prefer to attach to the surface of solid sulfur particles when oxidizing elemental sulfur for energy. Therefore, the detachment of *A. ferrooxidans* CP9 from active carbon might be due to the change of energy source from ferrous iron to sulfur for survival.

PCR-DGGE was used to examine the bacterial compositions and to analyze the variations in microbe communities. The DGGE bands were generated by 16S rRNA gene PCR amplification corresponding to 567 bp in length and were analyzed by DGGE electrophoresis during the 356 d of operation. Five samples were collected from the bioreactor at stage 1 (day 5), stage 2 (day 50), stage 4 (day 150), stage 6 (day 280), and stage 7 (day 350). The discernible bands were excised and sequenced (Table 1). Five bands were classified into three different eubacterial phyla. Bands A and C showed homology to the inoculated *A. ferrooxidans* with 99% similarity and were grouped under Phylum *Proteobacteria*. Band C was considered

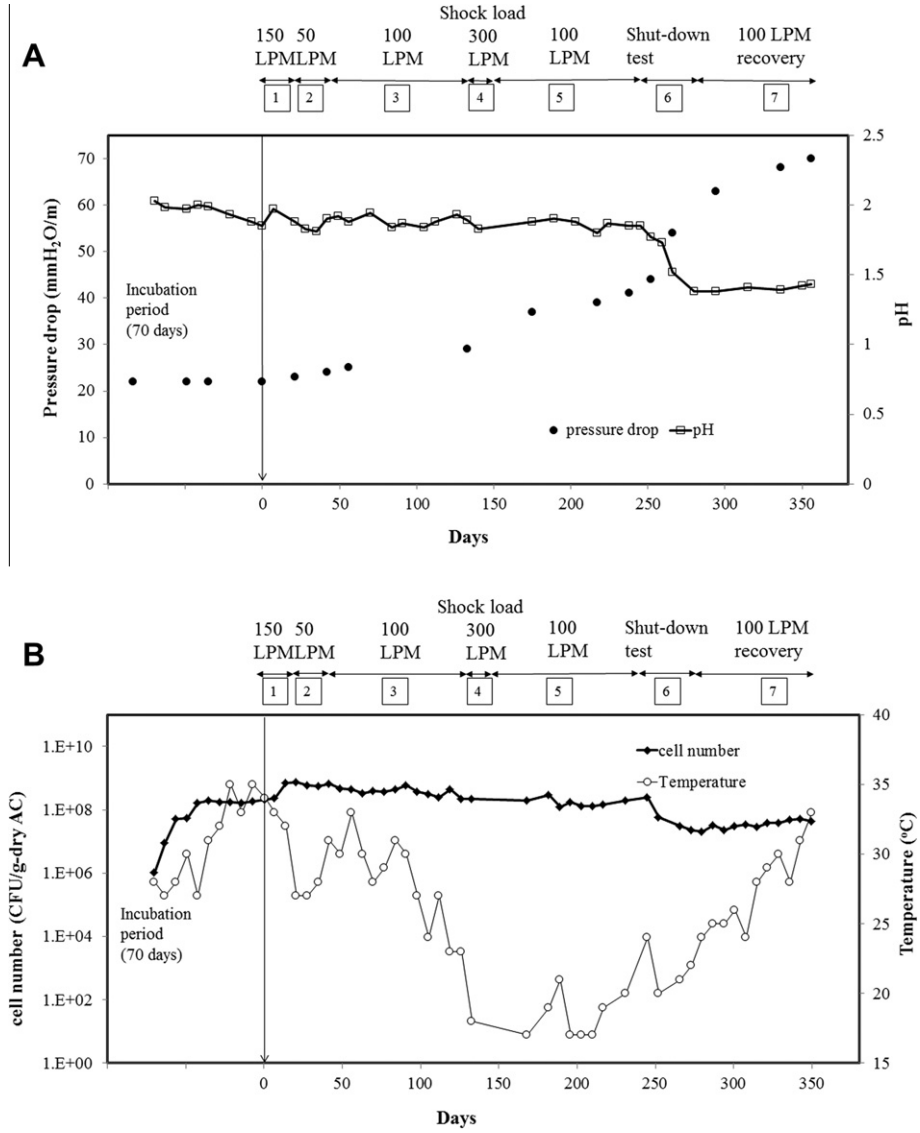

Fig. 5. Effects of pressure drop, pH and cell density on the system performance. (A) Pressure drop and pH variation profiles at each stage. The system was operated after microbial immobilization process of 70 d. (B) Cell density and medium temperature profiles in the biological reactor.

as an exotic subspecies of *A. ferrooxidans* that was different from the inoculation strain and appeared early in the operation. Band B was clustered within the phylum *Nitrospirae* and showed 99% similarity to *L. ferriphilum*. Bands D and E were designated under the phylum *Firmicutes* and showed 100% and 98% similarity to *Sulfobacillus* sp. L15 and *S. thermosulfidooxidans*, respectively. These exotic bacteria had the same features of growing in acidophilic conditions, autotrophic growth (*Sulfobacillus* sp. was mixotrophic), metal tolerance, and can obtain the reducing power by ferrous iron oxidation.

The relative abundance of *A. ferrooxidans* was 100% dominant in stage 1, but dropped to 78% in stage 2 because of the presence of *L. ferriphilum*. The relative amount of *L. ferriphilum* was not stable and increased with the decrease of H_2S loading in the system. This finding contrasted with that of *A. ferrooxidans*. Rawlings et al. (1999) reported that the main factor for bacterial growth to dominate biooxidation processes for the two strains is the ratio of ferric to ferrous iron (redox potential). During the high ferric iron stages (stages 2 and 6), *L. ferriphilum* was less affected because of the strong ferric iron resistance. However, in the high ferrous iron

Table 1
Nucleotide sequence similarity and relative amount of sequenced DGGE bands at stage 1 (day 5), stage 2 (day 50), stage 4 (day 150), stage 6 (day 280), and stage 7 (day 350).

Band	Closest relatives	Accession number	Similarity (%)	Relative abundance of DGGE bands (%)				
				Stage				
				1	2	4	6	7
A	*Acidithiobacillus ferrooxidans*	AF362022	100	81.2	70.2	78.2	42.3	43.2
B	*Leptospirillum ferriphilum*	JF510470	99	0	14.3	9.4	29.2	5.7
C	*Acidithiobacillus ferrooxidans*	JN224813	99	18.8	7.7	10.7	9.8	4.3
D	*Sulfobacillus* sp. L15	AY007663	100	0	3.5	0.9	16.2	46.8
E	*Sulfobacillus thermosulfidooxidans*	EU499919	98	0	4.3	0.8	2.5	0

stages (stages 4 and 7), *L. ferriphilum* was not able to compete with *A. ferrooxidans* due to the low redox potential in the media. This phenomenon properly elucidated the variation of the relative amount of *L. ferriphilum* in this long-term H_2S elimination operation.

Additionally, Johnson et al. (2005) showed that *Sulfobacillus* sp. is moderately thermophilic and gains reducing power from ferrous iron or mineral sulfide oxidation, which is similar to that of the inoculated *A. ferrooxidans* CP9. The relative amount of *Sulfobacillus* sp. dramatically increased to 46% in stage 7 compared with previous stages. Yahya and Johnson (2002) found that *Sulfobacillus* sp. had good iron oxidation activity at pH 1.2 compared with *A. ferrooxidans* and *L. ferrooxidans*. However, no ferrous oxidation was detected from the two latter strains in the same conditions. Therefore, in our operation, the decrease of pH to 1.38 during the shutdown period was the major factor that favored the increase of *Sulfobacillus* sp. In addition, the presence of *Sulfobacillus* sp. also contributed to the maintenance of oxidation ability of the bioreactor in stage 7. Although the *A. ferrooxidans* cell count gradually decreased from 100% in stage 1 to 47.5% in stage 7 because of the appearance of exotic bacteria after the shutdown test, the cell count was stably maintained above 5×10^7 CFU/g-AC during the operation (Fig. 5B).

Comparing the culture pH of these bacteria, the growth of *L. ferrooxidans* and *Sulfobacillus* sp. were more acidophilic than that of *A. ferrooxidans* (Yahya et al., 1999). In several bioleaching processes, for the purpose of avoiding the formation of jarosite, *L. ferrooxidans* or *Sulfobacillus* sp. were used instead of *A. ferrooxidans* in the biotic reaction to regenerate the oxidant ferric iron in extremely low pH. Jarosite is deposited on the surfaces of sulfide minerals, which impedes ferrous iron oxidation (Yahya and Johnson, 2002). However, in the H_2S elimination system, the chemical reaction efficiency of H_2S oxidation by ferric iron decreased with pH drop. Thus, considering both high H_2S removal rate and avoidance of jarosite formation, the choice of *A. ferrooxidans* growing between pH 2–2.5 was employed as the optimal operation conditions. Therefore, overall, the system was robust, and the inoculated *A. ferrooxidans* could maintain a high population after long-term field operation.

Compared with the biological methods for the direct oxidation of H_2S by microbes, this system can tolerate high concentrations of H_2S without the consequent pH drop attributed to sulfate accumulation. The results demonstrate the robust performance of the chemical–biological system during the operation period with stable parameters. In addition, the number of chemical absorbers could be adjusted for optimal H_2S removal. Therefore, this combined system can be applied for industrial processes with high concentrations of H_2S (e.g., above 1%) emission.

4. Conclusions

A chemical–biological H_2S removal process was established for pilot-scale biogas purification. The average inlet H_2S concentration was 3542 ppm, and 90–95% removal efficiency was achieved under GRT between 288 to 144 s (biogas flow rate between 50 to 100 LPM). The purified biogas with less than 150 ppm residual H_2S was burned for power generation. The system showed great recovery ability within 16 d after shock loading and shutdown test without permanent damage. Hence, the chemical–biological system is feasible for biogas purification and power generation.

Acknowledgements

The work was financially supported by grants NSC 100-3114-B-009-001 from the National Science Council and by the Aim for the Top University Plan of the National Chiao Tung University and Ministry of Education, Taiwan.

References

Belmabkhout, Y., De Weireld, G., Sayari, A., 2009. Amine-bearing mesoporous silica for CO_2 and H_2S removal from natural gas and biogas. Langmuir 25, 13275–13278.

Chiu, S.-Y., Kao, C.-Y., Huang, T.-T., Lin, C.-J., Ong, S.-C., Chen, C.-D., Chang, J.-S., Lin, C.-S., 2011. Microalgal biomass production and on-site bioremediation of carbon dioxide, nitrogen oxide and sulfur dioxide from flue gas using *Chlorella* sp. cultures. Bioresource Technology 102, 9135–9142.

Chung, Y.-C., Ho, K.-L., Tseng, C.-P., 2007. Two-stage biofilter for effective NH_3 removal from waste gases containing high concentrations of H_2S. Journal of the Air & Waste Management Association 57, 337–347.

Chung, Y.C., Ho, K.L., Tseng, C.P., 2006. Treatment of high H_2S concentrations by chemical absorption and biological oxidation process. Environmental Engineering Science 23, 942–953.

Daoud, J., Karamanev, D., 2006. Formation of jarosite during Fe^{2+} oxidation by *Acidithiobacillus ferrooxidans*. Minerals Engineering 19, 960–967.

Dave, S.R., 2008. Selection of *Leptospirillum ferrooxidans* SRPCBL and development for enhanced ferric regeneration in stirred tank and airlift column reactor. Bioresource Technology 99, 7803–7806.

Demirbas, A., 2010. Methane Gas Hydrate (Green Energy and Technology), 1st ed. Springer.

Deng, L., Chen, H., Chen, Z., Liu, Y., Pu, X., Song, L., 2009. Process of simultaneous hydrogen sulfide removal from biogas and nitrogen removal from swine wastewater. Bioresource Technology 100, 5600–5608.

Ebrahimi, S., Kleerebezem, R., van Loosdrecht, M., Heijnen, J., 2003. Kinetics of the reactive absorption of hydrogen sulfide into aqueous ferric sulfate solutions. Chemical Engineering Science 58, 417–427.

Gabriel, D., 2003. Retrofitting existing chemical scrubbers to biotrickling filters for H_2S emission control. Proceedings of the National Academy of Sciences 100, 6308–6312.

Giaveno, A., Lavalle, L., Guibal, E., Donati, E., 2008. Biological ferrous sulfate oxidation by *A. ferrooxidans* immobilized on chitosan beads. Journal of Microbiological Methods 72, 227–234.

Giro, M.E.A., Garcia Jr., O., Zaiat, M., 2006. Immobilized cells of *Acidithiobacillus ferrooxidans* in PVC strands and sulfite removal in a pilot-scale bioreactor. Biochemical Engineering Journal 28, 201–207.

González-Sánchez, A., Revah, S., Deshusses, M.A., 2008. Alkaline biofiltration of H_2S odors. Environmental Science & Technology 42, 7398–7404.

He, H., Zhang, C.-G., Xia, J.-L., Peng, A.-A., Yang, Y., Jiang, H.-C., Zheng, L., Ma, C.-Y., Zhao, Y.-D., Nie, Z.-Y., Qiu, G.-Z., 2008. Investigation of elemental sulfur speciation transformation mediated by *Acidithiobacillus ferrooxidans*. Current Microbiology 58, 300–307.

Ho, K.-L., Chung, Y.-C., Lin, Y.-H., Tseng, C.-P., 2008. Microbial populations analysis and field application of biofilter for the removal of volatile-sulfur compounds from swine wastewater treatment system. Journal of Hazardous Materials 152, 580–588.

Jiang, X., Yan, R., Tay, J.H., 2009. Simultaneous autotrophic biodegradation of H_2S and NH_3 in a biotrickling filter. Chemosphere 75, 1350–1355.

Johnson, D.B., Okibe, N., Hallberg, K.B., 2005. Differentiation and identification of iron-oxidizing acidophilic bacteria using cultivation techniques and amplified ribosomal DNA restriction enzyme analysis. Journal of Microbiological Methods 60, 299–313.

Kucera, J., Bouchal, P., Cerna, H., Potesil, D., Janiczek, O., Zdrahal, Z., Mandl, M., 2011. Kinetics of anaerobic elemental sulfur oxidation by ferric iron in *Acidithiobacillus ferrooxidans* and protein identification by comparative 2-DE-MS/MS. Antonie van Leeuwenhoek 101, 561–573.

Malhotra, S., Tankhiwale, A.S., Rajvaidya, A.S., Pandey, R.A., 2002. Optimal conditions for bio-oxidation of ferrous ions to ferric ions using *Thiobacillus ferrooxidans*. Bioresource Technology 85, 225–234.

Mesa, M., Andrades, J., Macias, M., Cantero, D., 2004. Biological oxidation of ferrous iron: study of bioreactor efficiency. Journal of Chemical Technology & Biotechnology 79, 163–170.

Mesa, M., Macias, M., Cantero, D., 2002. Biological iron oxidation by *Acidithiobacillus ferrooxidans* in a packed-bed bioreactor. Chemical and Biochemical Engineering Quarterly 16, 69–73.

Nielsen, A.H., Hvitved-Jacobsen, T., Vollertsen, J., 2008. Effects of pH and iron concentrations on sulfide precipitation in wastewater collection systems. Water Environment Research 80, 380–384.

Nizami, A.S., Murphy, J.D., 2010. What type of digester configurations should be employed to produce biomethane from grass silage? Renewable and Sustainable Energy Reviews 14, 1558–1568.

Omri, I., Bouallagui, H., Aouidi, F., Godon, J.-J., Hamdi, M., 2011. H_2S gas biological removal efficiency and bacterial community diversity in biofilter treating wastewater odor. Bioresource Technology 102, 10202–10209.

Pagella, C., De Faveri, D., 2000. H_2S gas treatment by iron bioprocess. Chemical Engineering Science 55, 2185–2194.

Park, D., Lee, D.S., Joung, J.Y., Park, J.M., 2005. Comparison of different bioreactor systems for indirect H_2S removal using iron-oxidizing bacteria. Process Biochemistry 40, 1461–1467.

Peiffer, S., Gade, W., 2007. Reactivity of ferric oxides toward H_2S at low pH. Environmental Science & Technology 41, 3159–3164.

Ramírez, M., Fernández, M., Granada, C., Le Borgne, S., Gómez, J.M., Cantero, D., 2011. Biofiltration of reduced sulphur compounds and community analysis of sulphur-oxidizing bacteria. Bioresource Technology 102, 4047–4053.

Rasi, S., Veijanen, A., Rintala, J., 2007. Trace compounds of biogas from different biogas production plants. Energy 32, 1375–1380.

Rawlings, D.E., Tributsch, H., Hansford, G.S., 1999. Reasons why "*Leptospirillum*-"like species rather than *Thiobacillus ferrooxidans* are the dominant iron-oxidizing bacteria in many commercial processes for the biooxidation of pyrite and related ores. Microbiology 145, 5–13.

Sharma, P., 2003. Surface characterization of *Acidithiobacillus ferrooxidans* cells grown under different conditions. Hydrometallurgy 71, 285–292.

Soreanu, G., Falletta, P., Béland, M., Edmonson, K., Ventresca, B., Seto, P., 2010. Empirical modelling and dual-performance optimisation of a hydrogen sulphide removal process for biogas treatment. Bioresource Technology 101, 9387–9390.

Tanaka, Y., 2002. A dual purpose packed-bed reactor for biogas scrubbing and methane-dependent water quality improvement applying to a wastewater treatment system consisting of UASB reactor and trickling filter. Bioresource Technology 84, 21–28.

Yahya, A., Johnson, D., 2002. Bioleaching of pyrite at low pH and low redox potentials by novel mesophilic Gram-positive bacteria. Hydrometallurgy 63, 181–188.

Yahya, A., Roberto, F., Johnson, D., 1999. Novel mineral-oxidizing bacteria from Montserrat (WI): physiological and phylogenetic characteristics. Process Metallurgy 9, 729–739.

Yarzabal, A., 2004. Regulation of the expression of the *Acidithiobacillus ferrooxidans rus* operon encoding two cytochromes c, a cytochrome oxidase and rusticyanin. Microbiology 150, 2113–2123.